

Investigation of the Effects of Thermal Cycling and Surface Treatments on Interim Resin Materials Produced with Additive Manufacturing

GOKNUR OZTURK¹, DEGER ONGUL^{2*}

¹ Istanbul University, Institute of Graduate Studies in Health Sciences, Department of Prosthodontics, Istanbul University, 34452 Beyazit, İstanbul-Türkiye

² Istanbul University, Faculty of Dentistry, Department of Prosthodontics, Istanbul University, 34452 Beyazit, İstanbul-Türkiye

Abstract: *This study aimed to compare the impact of thermal cycling on the flexural strength (σ_f) of 3-dimensional (3D) printer resins and polymethyl methacrylate (PMMA). It also aimed to evaluate different surface treatment protocols and surface sealant applications on the surface roughness (Ra) and surface hardness (VHN) of the resins used. Rectangular (25×2×2 mm) and disc (Ø10×2-mm) specimens were fabricated from auto-polymerized PMMA, and 3D-printed resins were tested for mechanical properties (ISO 10477) using thermal cycling (n=10). Disc specimens were separated into three groups (n=10) based on the surface treatments: conventional sanding (C), disk polishing (P), and surface sealant coating (O). Ra and VHN values were statistically analyzed with the Kolmogorov Smirnov, Shapiro Wilk, Independent Samples t-test, Mann-Whitney test, one-way ANOVA test and Kruskal Wallis test ($\alpha = .05$). A significant main effect was found on the flexural strength analysis for each of the two factors: thermal cycling procedure ($p < 0.001$) and materials ($p < 0.001$). A significant main effect was found on the surface roughness and hardness analysis for each of the two factors: surface treatment protocols ($p < 0.001$) and materials ($p < 0.001$). Based on the results; interim materials produced with 3D-printed resins have better mechanical properties than conventionally polymerized materials. Coated materials had lower surface roughness values than polished ones, and adding a surface sealant agent increased their hardness significantly.*

Keywords: *additive manufacturing, flexural strength, interim prosthesis, 3D printed resin*

1. Introduction

Interim fixed prostheses protect the prepared teeth and periodontal tissues while ensuring oral function and aesthetics [1-5]. Their characteristics play a significant role in determining the success of the final restorations [6, 7]. Different materials and methods aim to produce interim restorations that are aesthetically pleasing, easy to produce, and exhibit high strength and hardness [8-12]. Although acrylic resins are cost-effective and can be polished, they can experience challenges due to exothermic reactions and shrinkage [13, 14]. Computer-aided design and manufacturing (CAD-CAM) techniques have enhanced the quality of interim restorations, providing improved precision, better fit, and fewer discrepancies than traditional methods [15-18]. The 3D printing is a different method for digitally producing interim restorations. Its benefits include simple production steps, lower cost, minimal waste material, and reduced fabrication time [19-22]. The aesthetic properties [23-25], biocompatibility [26-29], microbial adhesion [30, 31], and mechanical characteristics [32-35] of additive manufacturing (AM) interim restorations are influenced by printer technology, resin composition, printing parameters, and post-processing methods [28, 29, 36-38].

The literature includes studies assessing interim restorative materials' mechanical properties and surface roughness [31, 33]. However, there is limited information regarding the effects of thermocycling on flexural strength and surface treatment protocols on surface properties [19, 39]. Therefore, the null hypotheses were that there would be no differences in σ_f values among the tested interim materials, that

*email: dongul@istanbul.edu.tr

thermal cycling would not affect these parameters, and that resin type and surface treatment protocols would not influence surface roughness and Vickers hardness.

2. Materials and methods

2.1. Specimen preparation

Disc (n=120) and rectangular-shaped specimens (n=80) were prepared by using auto-polymerized PMMA and three different printed resin interim materials. The specimens were designed as rectangular (25×2×2 mm) and disc (Ø10×2-mm) using 3D printer (Asiga Max; Asiga) software and saved as an STL file. Specimens were printed with the same printer from 3D resin materials (BegoVarseo Smiletemp; Bego, Optiprint Lumina; Dentona, Power Rezin; 3BFAB). Ultrasonic baths of the specimens were completed by the manufacturer's instructions. After the initial polymerization, the specimen was exposed to ultraviolet light in a polymerization unit (S2; DWS) for 20 min to achieve its final properties. 3D-printed rectangular and disc specimens were removed from the support structures to produce the conventional group with silicone molds. Conventional PMMA (Imident; Imicryl) was mixed according to the manufacturer's instructions, poured into the silicone mold cavity, and polymerization was carried out. All specimens were sanded with silicon carbide abrasive papers (360, 600 sic) under constant water irrigation for 15 s. The rectangular specimens from each material were divided into two groups (n=10) based on different thermal cycling (DTS B1, Dentester, Salubris Technica): 0 cycles (NA), 2500 cycles (A). The thermocycler's distilled water baths were set to 5°C and 55°C, with a transport time of 20 seconds and a dwell time of 15 s.

Disc-shaped specimens were grouped (n=10) by surface treatment: Group C had no post-sanding treatment, Group P was polished with Clearfil Twist Dia (Kuraray) after sanding, and Group O received a single layer of sealant (Optiglaze; GC) polymerized for 30 s with a Planmeca Lumion LED (Mectron).

The three-point flexural strengths of the specimens were measured using an Instron Model 8501 (Instron Corp) universal testing machine with a 0.5-kN load cell. A load was applied at a 1 mm/min crosshead speed until fracture occurred. The load at failure was recorded, and flexural strength (σ in MPa) was calculated using the following formula:

$$\sigma = 3F_{\max}L / 2bd^2$$

where F_{\max} is the fracture strength, L is the length, b is the with, and d is the thickness of the specimens [40]. A contact profilometer (Surtronic 25; Taylor Hobson) was used to measure each specimen's roughness (R_a). The disc specimens' surface microhardness was evaluated using a microhardness test device (Innovatest; Borgharenweg). To measure the Vickers hardness value of each specimen, a 490 N load was applied for 15 s, and a rhombus-shaped indentation was obtained on the specimen surface. The longest diagonal of the diamond trace was marked. Mean was calculated from three repeated measurements on the same specimen. Scanning electron microscope (SEM) images of the disc specimens were obtained from the subgroup specimens at ×1000 magnification (FEI Versa 3D Dual Beam). Before imaging, the sample surfaces were coated with gold by sputtering using a gold coating device (OptoSense).

2.2. Statistical analyses

Statistical analyses were performed using a software program (Statistical Package for the Social Sciences; SPSS 21.0 Software). Compliance of numerical variables with normal distribution was evaluated using visual and analytical methods (Kolmogorov Smirnov and Shapiro Wilk test). In pairwise comparison, the Independent Samples t-test was used when the data followed a normal distribution, and the Mann-Whitney U test was used when the data were determined as unnormally distributed. In comparing more than two groups with continuous numerical variables, the 1-way ANOVA test was used when the data followed a normal distribution, and the Kruskal Wallis test was used when the data were determined as unnormally distributed. If necessary, Tukey's HSD (post-doc) analysis was performed,

and pairwise comparisons were evaluated with Bonferroni correction. The relationship between numerical variables was examined with Spearman and Pearson correlation tests ($\alpha = .05$)

3. Results and discussions

3.1. Flexural strength tests

Figure 1 and Table 1 display flexural strength values and the combination of thermal cycling periods for each group. Statistical tests showed significant differences in flexural strength within the group during thermal cycling ($p < 0.05$). Conventional PMMA had the lowest mean flexural strength values among the thermal cycled resin materials ($p < 0.001$). The flexural strength of the thermal cycled Bego groups were statistically significantly higher than all groups ($p < 0.001$).

Table 1. Flexural strength (σ_{fs}) values computed among different subgroups tested

Test protocol	Group Code	Mean	Std. Deviation	Median	Minimum	Maximum
Flexural strength	Group Bego NA	118.57	8.97	117.64	107.58	131.25
	Group Bego A	83.05	8.04	86.02	71.33	92.81
	Group Optiprint NA	93.55	8.25	89.25	87.04	109.61
	Group Optiprint A	63.62	3.96	62.69	57.66	70.01
	Group Power NA	82.64	2.6	82.33	79.61	88.37
	Group Power A	55.33	1.76	54.63	53.41	57.94
	Group Conventional PMMA NA	70.14	4.09	68.55	65.75	78.71
	Group Conventional PMMA A	45.74	3.01	45.97	41.62	49.63

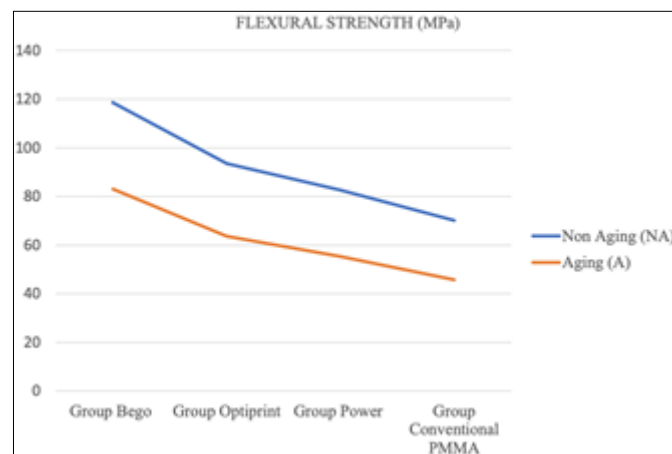


Figure 1. Schematic drawing of the flexural strengths of the groups

Both null hypotheses were rejected, showing that the tested materials impacted their mechanical and surface properties. Flexural strength changed with thermal cycling, while various surface treatment protocols affected the roughness and hardness of interim materials. Although the flexural strength test may not fully replicate the dynamic oral environment, it offers a reliable comparison of dental materials' mechanical properties under controlled conditions [2]. Thus, this study used flexural strength testing to evaluate the materials' mechanical parameters.

In the current study, conventional PMMA resin exhibited lower flexural strength than 3D-printed resins. Conventional PMMA resins consist of mono-functional, low molecular-weight, linear molecules contributing to reduced strength and rigidity. Furthermore, air bubbles can become trapped if not polymerised under pressure, decreasing strength [35]. Consequently, the presence of air bubbles and variations in chemical composition likely resulted in lower flexural strength values for conventional PMMA resin compared to 3D-printed resin specimens.

Due to the high cost and time associated with clinical studies, in vitro laboratory simulations are commonly conducted. Thermal cycling is a standard method for simulating aging in controlled lab

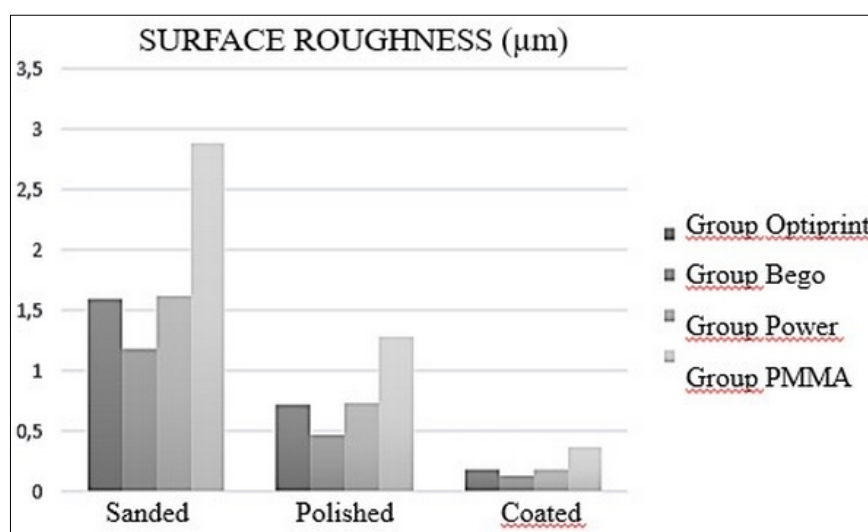
settings [32]. In this study, conventional PMMA exhibited significantly lower σ_f values (45.74 ± 3 MPa) during thermal cycling. The reduced polymerization of conventional materials may result in increased water absorption, potentially leading to a plasticizing effect on the polymer networks and a subsequent reduction in strength [35]. These findings align with previous studies that indicated conventional PMMA resins have lower mean σ_f values than 3D-printed resins [19, 33, 34]. The flexural strength of 3D-printed materials declined due to residual stress from water absorption and temperature changes, leading to weakened interlayer bonds and potential long-term structural failure [38]. In a study by Scotti et al. [19], 3D-printed materials showed superior flexural strength compared to PMMA, aligning with our findings. The current study observed differences in the flexural strengths of 3D-printed resins with different filler contents after thermal cycling. It could be argued that the manufacturing process is not the sole factor influencing the mechanical properties of materials; other contributing factors may include various chemical compositions and different filler contents of interim materials. Kebler et al. [37] compared the flexural strength of different filler contents in 3D-printed resins. Consistent with the present study's findings, the authors mentioned that the varying filler content influences the flexural strength in the chemical composition of the tested material.

3.2. Surface roughness test

The mean \pm standard deviation values of Ra for the different interim material and surface treatment method combinations have been detailed in Table 2. Significant differences were found with the same surface treatment protocols applied to the different interim materials ($p < 0.001$) (Figure 2).

Table 2. Surface roughness (Ra) values computed among different subgroups tested.

Test protocol	Group Code	Mean \pm SD	Std. Deviation	Median	Minimum	Maximum
Surface Roughness (Ra)	Group Bego C	1.18	± 0.04	1.18	1.12	1.23
	Group Bego P	0.47	± 0.1	0.44	0.37	0.65
	Group Bego O	0.13	± 0.02	0.13	0.11	0.16
	Group Optiprint C	1.59	± 0.12	1.56	1.45	1.77
	Group Optiprint P	0.72	± 0.04	0.73	0.62	0.77
	Group Optiprint O	0.19	± 0.01	0.2	0.17	0.21
	Group Power C	1.62	± 0.06	1.62	1.5	1.71
	Group Power P	0.73	± 0.05	0.73	0.65	0.8
	Group Power O	0.19	± 0.02	0.2	0.17	0.21
	Group Conventional PMMA C	2.87	± 0.08	2.88	2.74	2.99
	Group Conventional PMMA P	1.29	± 0.09	1.3	1.09	1.4
	Group Conventional PMMA O	0.37	± 0.02	0.37	0.33	0.39



A

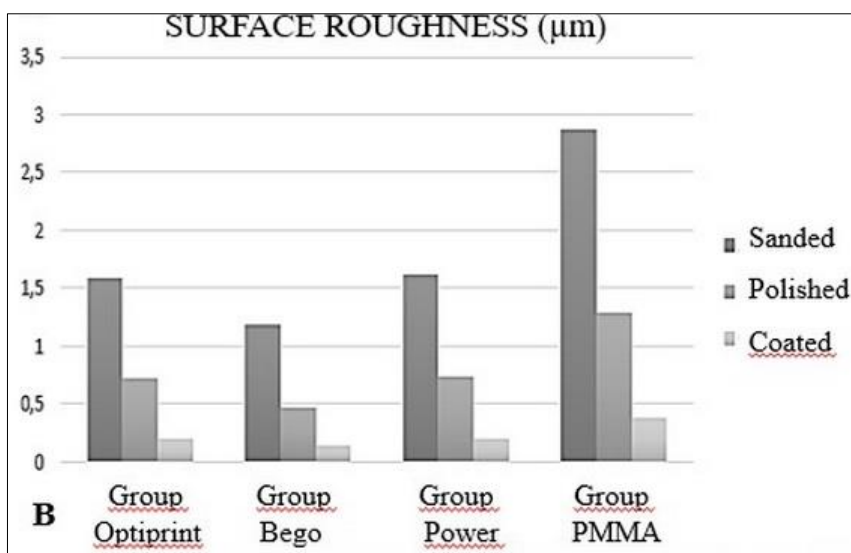


Figure 2. Schematic drawing of the surface roughness of the groups

A. Effect of surface treatment protocol on surface roughness

B. Effect of different surface treatment protocols on surface roughness of interim material

According to Tukey’s HSD and Bonferroni correction, the conventional PMMA group showed the highest surface roughness among all interim groups, regardless of surface treatments ($p < 0.001$). The Bego resin group showed the lowest surface roughness among all interim groups in this study, regardless of surface treatment protocols ($p < 0.001$). Significant differences in Ra values were observed with various surface treatment protocols ($p < 0.001$). The coated groups exhibited significantly lower Ra values when compared to the conventionally polished groups treated with a surface sealant ($p < 0.001$).

3.3. Surface hardness test

Table 3 presents the mean \pm standard deviation values of VHN for the various combinations of interim materials and surface treatment protocols. Statistically significant differences were observed with consistent surface treatment protocols across different interim materials ($p < 0.001$) (Figure 3). The conventional PMMA group, regardless of the surface treatments, showed the lowest surface hardness ($p < 0.001$).

Table 3. Vickers hardness (VHN) values of the subgroups tested

Test protocol	Group Code	Mean \pm SD	Std. Deviation	Median	Minimum	Maximum
Vickers hardness (VHN)	Group Bego C	25.07	± 0.9	25.84	24.26	26.85
	Group Bego P	29.17	± 0.49	28.99	28.52	29.87
	Group Bego O	35.02	± 0.68	35.26	33.96	35.83
	Group Optiprint C	21.92	± 0.82	21.78	20.89	22.95
	Group Optiprint P	26.27	± 0.99	26.33	24.82	27.82
	Group Optiprint O	30.94	± 1.22	30.55	29.46	32.62
	Group Power C	21.55	± 1.11	21.86	19.81	22.75
	Group Power P	25.55	± 0.64	25.78	24.61	26.34
	Group Power O	29.03	± 0.92	29.03	27.28	30.35
	Group Conventional PMMA C	19.18	± 1.72	19.51	16.41	21.19
	Group Conventional PMMA P	22.01	± 1.36	22.37	19.69	23.52
	Group Conventional PMMA O	24.71	± 0.65	24.96	23.32	25.42

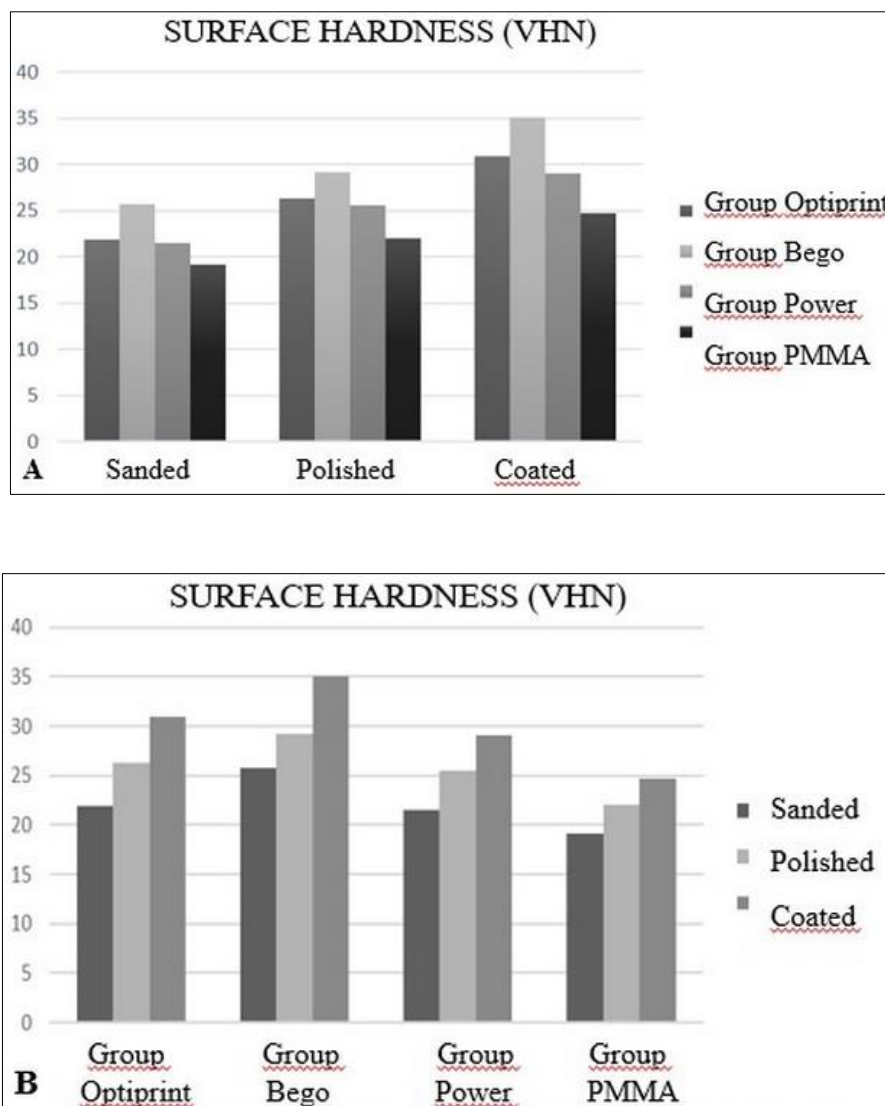


Figure 3. Schematic drawing of the surface hardness of the groups

A. Effect of different surface treatment protocols on surface hardness.

B. Effect of different surface treatment protocols on surface hardness of interim material

The Bego resin group showed the highest surface hardness in all surface treatment groups. Significant differences were found in the VHN results when different surface treatment protocols were applied to the same groups ($p < 0.001$). The groups coated with sealant exhibited significantly higher surface hardness values compared to the other surface treatment groups ($p < 0.001$).

There was a strong negative correlation between the measurements of roughness and hardness for the groups that had the surface sanded, polished, and coated with surface sealant. ($r = -0.939$, $r = -0.974$, $r = -0.887$, $p < 0.001$).

This in vitro study examined the impact of different surface treatment protocols on the roughness and hardness of interim materials made from conventional PMMA and 3D-printed resin. Assessing the roughness of interim restorations is crucial for periodontal health, as roughness above $0.2 \mu\text{m}$ can enhance bacterial colonization, with $10 \mu\text{m}$ being the maximum clinically acceptable roughness [3, 4]. In this study, the R_a values for coated materials ranged from $0.13 \mu\text{m}$ to $0.37 \mu\text{m}$, all remaining below the unacceptable threshold of $10 \mu\text{m}$. Conventional PMMA exhibited higher surface roughness than 3D-printed resins across all treatment protocols, likely due to differences in chemical composition. Previous

studies have similarly found that conventional PMMA had the highest Ra values [21, 31]. Notably, the 3D-printed Bego group showed the lowest Ra values among the materials tested. Rizante et al. [24] also reported lower surface roughness in 3D-printed resins compared to conventional PMMA, aligning with the findings of this study that the chemical composition of the interim materials influences surface roughness.

Conventional polishing procedures can introduce additional surface defects and diminish the quality of interim restoration materials [7, 9]. However, applying a surface sealant has enhanced surface quality by filling microdefects through capillary action [9]. Applying a surface sealant to all interim materials significantly reduced surface roughness in this study. Shenoy et al. [17] compared various surface treatment protocols and found that groups treated with a surface sealant exhibited lower Ra values, aligning with our findings. Additionally, SEM images obtained in this study confirmed that applying a surface sealant effectively reduced surface roughness across all groups.

It is necessary to evaluate mechanical properties to evaluate new technologies and obtain the optimum material and a suitable technique for producing long-term interim restorations. One of these properties is flexural strength, and the other is microhardness [5]. A decrease in microhardness may indicate superficial degradation, leading to increased roughness, plaque accumulation, and reduced restoration lifespan [10]. In this current study, the 3D-printed resin showed significantly higher microhardness than conventional PMMA, regardless of surface treatment protocols, and this could be attributed to the different chemical compositions of the interim materials. Digholkar et al. [18] compared the surface hardness of the 3D-printed resin with PMMA. Their findings align with the current study, showing that the 3D-printed group had higher surface hardness due to cross-linked monomers and inorganic fillers, which enhanced wear resistance and minimized polymerization shrinkage. Previous studies have assessed how surface treatment protocols influence the surface roughness and hardness of interim materials [10, 11]. Comparing surface hardness after applying various treatments to the same material yielded different microhardness values, suggesting that these protocols expose harder regions of the material, thereby improving wear resistance. Olivera et al. [12] also examined the impact of surface treatment protocols on material hardness and found that these treatments significantly affected surface hardness values, aligning with the current study's findings. The current study found that all groups coated with surface sealant resin exhibited the highest surface hardness values compared to other groups. This improvement is attributed to the sealant's ability to enhance surface hardness by reducing the leaching of unpolymerized monomers. Thompson et al. [36] evaluated the impact of surface-coated materials on the Vickers hardness of PMMA-based interim materials and reported similar findings, with higher surface hardness values in the groups with coated surface sealants.

During the evaluation process, an increase in surface roughness leads to a decrease in surface hardness. SEM images revealed different surface characteristics among the groups tested, namely the C, P and O subgroups in Figure 4.

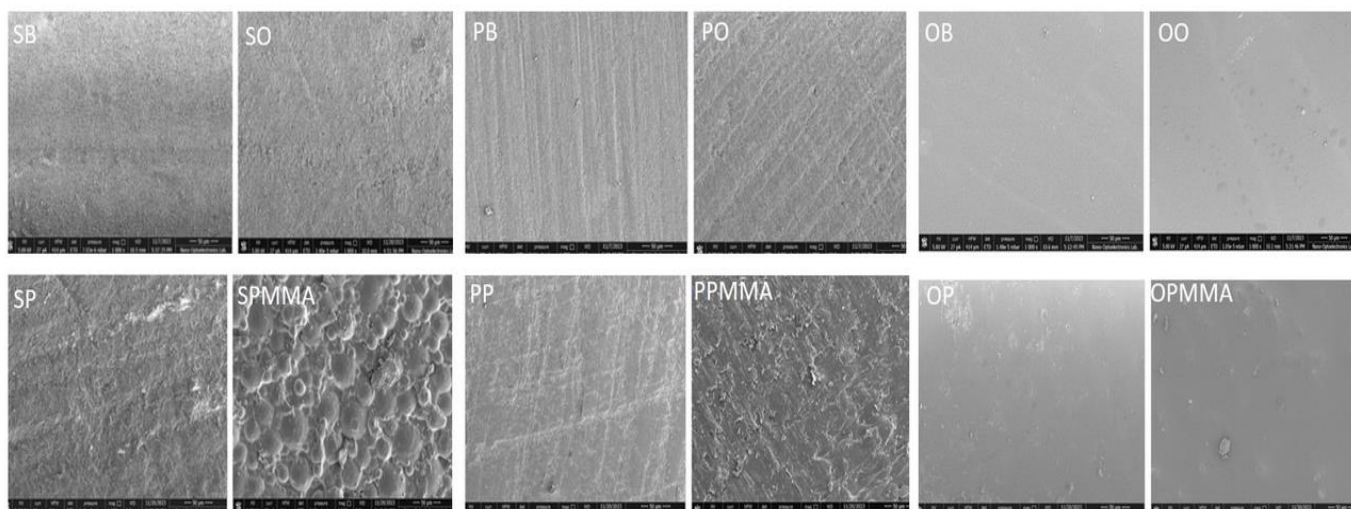


Figure 4. SEM images of the groups

SB. Sanded specimen of Bego group; **SO.** Sanded specimen Optiprint group;
SP. sanded specimen of Power group; **SPMMA.** sanded specimen of PMMA group;
PB. Polished specimen of Bego group; **PO.** Polished specimen of Optiprint group;
PP. Polished specimen of Power group; **PPMMA.** Polished specimen of PMMA group;
OB. Bego group coated with Optiglaze; **OO.** Optiprint group coated with Optiglaze;
OP. Power group coated with Optiglaze; **OPMMA.** PMMA group coated with Optiglaze

4. Conclusions

The limitations of this current study were that the interim materials' physical and mechanical properties were assessed under in vitro standardized conditions. Long-term clinical studies are required to evaluate different interim materials' clinical behaviour. Within the limitations of this study, it is concluded that both the type of interim material and the number of thermocycling periods affected flexural strength. 3D-printed resin exhibited superior mechanical properties to conventional PMMA, making it suitable for long-term interim restorations. The resin type significantly impacted the surface roughness and hardness of the interim materials, with 3D-printed resin showing better surface properties than conventional PMMA. Additionally, the application of a surface sealant markedly improved surface hardness and significantly reduced the surface roughness across all tested interim materials. Smoother surfaces facilitate cleaning, reducing plaque accumulation and periodontal risk. This underscores the importance of surface sealants in clinical practice to improve interim dental material efficacy.

References

1. GULER, A.U., YILMAZ, F., KULUNK, T., GULER, E., KURT, S., Effects of different drinks on stainability of resin composite provisional restorative materials, *J. Prosthet. Dent.*, 94, 2005, 118-124. <https://doi.org/10.1016/j.prosdent.2005.05.004>.
2. SHEN, C., RAWLS, H.R., ESQUIVEL-UPSHAW, J.F., Phillips' Science of Dental Materials, 12th ed. St. Louis: Elsevier - Health Sciences Division, 2021, p, 48-69.
3. BOLLEN, C.M., PAPAIOANNO, W., VAN ELDERE, J., SCHEPERS, E., QUIRYNEN, M., VAN STEENBERGHE, D, The influence of abutment surface roughness on plaque accumulation and peri-implant mucositis, *Clin. Oral. Implants. Res.*, 7, 1996, 201-211. <https://doi.org/10.1034/j.1600-0501.1996.070302.x>.
4. KAPLAN, B.A., GOLDSTEIN, GR., VIJAYARAGHAVAN, TV., NELSON, I.K., The effect of three polishing systems on the surface roughness of four hybrid composites: a profilometric and scanning electron microscopy study, *J. Prosthet. Dent.*, 76, 1996. 34-38. [https://doi.org/10.1016/S0022-3913\(96\)90343-1](https://doi.org/10.1016/S0022-3913(96)90343-1).

- 5.HASELTON, D.R., DIAZ-ARNOLD, A.M., VARGAS, M.A., Flexural strength of provisional crown and fixed partial denture resins, *J. Prosthet. Dent.*, 87, 2002, 225-228.
<https://doi.org/10.1067/mpr.2002.121406>.
- 6.SHIM, J.S., KIM, H.C., PARK, S.I., YUN, H.J., RYU, J.J., Comparison of various implant provisional resin materials for cytotoxicity and attachment to human gingival fibroblasts, *Int. J. Oral. Maxillofac. Implants.*, 34, 2019, 390-396. <https://doi.org/10.11607/jomi.6707>.
- 7.PATRAS, M., NAKA, O., DOUKOUDAKIS, S., PISSIOTIS, A., Management of provisional restorations' deficiencies: a literature review, *J. Esthet. Restor. Dent.*, 24, 2012, 26-38.
<https://doi.org/10.1111/j.1708-8240.2011.00467.x>.
- 8.HUAN, H., Machining characteristics and surface integrity of yttria stabilized tetragonal zirconia in high speed deep grinding, *J. Mater. Sci. Eng. A.*, 345, 2003, 155-163.
[https://doi.org/10.1016/S0921-5093\(02\)00466-5](https://doi.org/10.1016/S0921-5093(02)00466-5).
- 9.SARAC, D., SARAC, Y.S., KULUNK, S., URAL, C., KULUNK, T., The effect of polishing techniques on the surface roughness and color change of composite resins, *J. Prosthet. Dent.*, 96, 2006, 33-40. <https://doi.org/10.1016/j.prosdent.2006.04.012>.
- 10.BADRA, V.V., FARAONI, J.J., RAMOS, R.P., PALMA, R.G., Influence of different beverages on the microhardness and surface roughness of resin composites, *Oper. Dent.*, 30, 2005, 213-219.
- 11.CATELAN, A., BRISO, A.L., SUNDFELD, R.H., DOS SANTOS, P.H., Effect of artificial aging on the roughness and microhardness of sealed composites, *J. Esthet. Restor. Dent.*, 22, 2010, 324-330.
<https://doi.org/10.1111/j.1708-8240.2010.00360.x>.
- 12.SOLIMAN, H.A., ELKHOLANY, N.R., HAMAMA, H.H., EL-SHARKAWY, F.M., MAHMOUD, S.H., COMISI, J.C., Effect of different polishing systems on the surface roughness and gloss of novel nanohybrid resin composites, *Eur. J. Dent.*, 15, 2021, 259-265. I
<https://doi.org/10.1055/s-0040-1718477>
- 13.TURGUT, S., BAĞIS, B., AYDOĞAN AYAZ, E., ULUSOY, K.U., ALTINTAS, S.H., KORKMAZ, F.M., et al., Discoloration of provisional restorations after oral rinses, *Int. J. Med. Sci.*, 10, 2013, 1503-1509. <https://doi.org/10.7150/ijms.6647>.
- 14.HASELTON, D.R., DIAZ-ARNOLD, A.M., DAWSON, D.V., Effect of storage solution on surface roughness of provisional crown and fixed partial denture materials, *J. Prosthodont.*, 13, 2004, 227-232.
<https://doi.org/10.1111/j.1532-849X.2004.04039.x>.
- 15.PEREA-LOWERY, L., GIBREEL, M., VALLITTU, P.K., LASSILA, L., Characterization of the mechanical properties of CAD/CAM polymers for interim fixed restorations, *Dent. Mater. J.*, 39, 2020, 319-327. <https://doi.org/10.4012/dmj.2019-042>.
- 16.PENG, C.C., CHUNG, K.H., RAMOS, V. J.R., Assessment of the adaptation of interim crowns using different measurement techniques, *J. Prosthodont.*, 29, 2020, 87-93. <https://doi.org/10.1111/jopr.13122>.
- 17.SHENOY, A., RAJARAMAN, V., MAITI, S., Comparative analysis of various temporary computer-aided design/computer-aided manufacturing polymethyl methacrylate crown materials based on color stability, flexural strength, and surface roughness: An in vitro study, *J. Adv. Pharm. Technol. Res.*, 13, 2022, 130-135. https://doi.org/10.4103/japtr.japtr_119_22.
- 18.DIGHOLKAR, S., MADHAV, V.N.V., PALASKAR, J., Evaluation of the flexural strength and microhardness of provisional crown and bridge materials fabricated by different methods, *J. Indian. Prosthodont. Soc.*, 16, 2016, 328-334. <https://doi.org/10.4103/0972-4052.191288>.
- 19.SCOTTI, C.K., VELO, M.M.A.C., RIZZANTE, F.A.P., NASCIMENTO, T.R.L., MONDELLI, R.F.L., BOMBONATTI, J.F.S., Physical and surface properties of a 3D-printed composite resin for a digital workflow, *J. Prosthet. Dent.*, 124, 2020, 614.e1-5.
<https://doi.org/10.1016/j.prosdent.2020.03.029>.
- 20.PARK, G.S., KIM, S.K., HEO, S.J., KOAK, J.Y., SEO, D.G., Effects of printing parameters on the fit of implant-supported 3d printing resin prosthetics, *Materials (Basel)*, 12, 2019, 2533.
<https://doi.org/10.3390/ma12162533>.



21. GITI, R., DABIRI, S., MOTAMEDIFAR, M., DERAFFSHI, R., Surface roughness, plaque accumulation, and cytotoxicity of provisional restorative materials fabricated by different methods, *PLoS One*, 16, 2021, e0249551. <https://doi.org/10.1371/journal.pone.0249551>.
22. VAN NOORT, R., The future of dental devices is digital, *Dent. Mater.*, 28, 2012, 3-12. <https://doi.org/10.1016/j.dental.2011.10.014>.
23. REVILLA-LEÓN, M., UMORIN, M., ÖZCAN, M., PIEDRA-CASCÓN, W., Color dimensions of additive manufactured interim restorative dental material, *J. Prosthet. Dent.*, 123, 2020, 754-760. <https://doi.org/10.1016/j.prosdent.2019.06.001>.
24. RIZZANTE, F.A., BOMBONATTI, J.S., VASCONCELOS, L., PORTO, T.S., TEICH, S., MONDELLI, R.F., Influence of resin-coating agents on the roughness and color of composite resins, *J. Prosthet. Dent.* 122, 2019, 332.e1-5. <https://doi.org/10.1016/j.prosdent.2019.05.011>.
25. KÖROĞLU, A., SAHIN, O., DEDE, D.Ö., YILMAZ, B., Effect of different surface treatment methods on the surface roughness and color stability of interim prosthodontic materials, *J. Prosthet. Dent.*, 115, 2016, 447-455. <https://doi.org/10.1016/j.prosdent.2015.10.005>.
26. ALHARBI, N., OSMAN, R.B., WISMEIJER, D., Factors influencing the dimensional accuracy of 3D-printed full-coverage dental restorations using stereolithography technology, *Int. J. Prosthodont.*, 29, 2016, 503-510. <https://doi.org/10.11607/ijp.4835>.
27. AL-HUMOOD, H., ALFARAJ, A., YANG, C.C., LEVON, J., CHU, T.G., LIN, W.S., Marginal Fit, Mechanical Properties, and Esthetic Outcomes of CAD/CAM Interim Fixed Dental Prostheses (FDPs): A Systematic Review, *Materials.*, 16(5), 2023, 1996. <https://doi.org/10.3390/ma16051996>.
28. REVILLA-LEÓN, M., MEYERS, M.J., ZANDINEJAD, A., ÖZCAN, M., A review on chemical composition, mechanical properties, and manufacturing work flow of additively manufactured current polymers for interim dental restorations, *J. Esthet. Restor. Dent.*, 31, 2019, 51-57. <https://doi.org/10.1111/jerd.12438>.
29. REVILLA-LEÓN, M., MORILLO, J.A., ATT, W., ÖZCAN, M., Chemical composition, Knoop hardness, surface roughness, and adhesion aspects of additively manufactured dental interim materials, *J. Prosthodont.*, 30, 2021, 698-705. <https://doi.org/10.1111/jopr.13302>.
30. SHIM, J.S., KIM, J.E., JEONG, S.H., CHOI, Y.J., RYU, J.J., Printing accuracy, mechanical properties, surface characteristics, and microbial adhesion of 3D-printed resins with various printing orientations, *J. Prosthet. Dent.*, 124, 2020, 468-475. <https://doi.org/10.1016/j.prosdent.2019.05.034>.
31. RIBEIRO, A.K.C., FREITAS, R.F.C.P., CARVALHO, I.H.G., MIRANDA, L.M., SILVA, N.R., ALMEIDA, F.D., et al., Flexural strength, surface roughness, micro-CT analysis, and microbiological adhesion of a 3D-printed temporary crown material, *Clin. Oral. Investig.*, 27(5), 2023, 2207-2220. <https://doi.org/10.1007/s00784-023-04941-3>.
32. GALE, M.S., DARVELL, B.W., Thermal cycling procedures for laboratory testing of dental restorations, *J. Dent.*, 27, 1999, 89-99. [https://doi.org/10.1016/s0300-5712\(98\)00037-2](https://doi.org/10.1016/s0300-5712(98)00037-2).
33. TAŞIN, S., ISMATULLAEV, A., Comparative evaluation of the effect of thermocycling on the mechanical properties of conventionally polymerized, CAD-CAM milled, and 3D-printed interim materials, *J. Prosthet. Dent.*, 127, 2022, 173. <https://doi.org/10.1016/j.prosdent.2021.09.020>.
34. ELLAKANY, P., FOUUDA, S.M., MAHROUS, A.A., ALGHAMDI, M.A., ALY, N.M., Influence of CAD/CAM Milling and 3D-Printing Fabrication Methods on the Mechanical Properties of 3-Unit Interim Fixed Dental Prosthesis after Thermo-Mechanical Aging Process, *Polymers (Basel)*, 14, 2022, 4103. <https://doi.org/10.3390/polym14194103>.
35. BOARO, L.C., GONÇALVES, F., GUIMARÃES, T.C., FERRACANE, J.L., PFEIFER, C.S., BRAGA, R.R., Sorption, solubility, shrinkage and mechanical properties of “low-shrinkage” commercial resin composites, *Dent. Mater.*, 29, 2013, 398-404. <https://doi.org/10.1016/j.dental.2013.01.006>.
36. THOMPSON, G.A., LUO, Q., Contribution of postpolymerization conditioning and storage environments to the mechanical properties of three interim restorative materials, *J. Prosthet. Dent.*, 112, 2014, 638-648. <https://doi.org/10.1016/j.prosdent.2014.04.008>.



- 37.KEBLER, H., HICKEL, R., LLIE, N., In vitro investigation of the influence of printing direction on the flexural strength, flexural modulus and fractographic analysis of 3D-printed temporary materials, *Dent. Mater. J.*, 29, 2021, 641-649. <https://doi.org/10.4012/dmj.2020-147>.
- 38.TAHAYERI, A., MORGAN, M., FUGOLIN, A.P., BOMPOLAKI, D., ATHIRASALA, A., PFEIFER, C.S., et al., 3D printed versus conventionally cured provisional crown and bridge dental materials, *Dent. Mater.*, 34, 2018, 192-200. <https://doi.org/10.1016/j.dental.2017.10.003>.
- 39.REYMUS, M., FABRITIUS, R., KEBLER, A., HICKEL, R., EDELHOFF, D., STAWARCZYK, B., Fracture load of 3D-printed fixed dental prostheses compared with milled and conventionally fabricated ones: The impact of resin material, build direction, post-curing, and artificial aging-an in vitro study, *Clin. Oral. Investig.*, 24, 2020, 701-710. <https://doi.org/10.1007/s00784-019-02952-7>.
- 40.***International Organization for Standardization. ISO 10477:2018 dentistry - polymer-based crown and veneering materials. Available at: <https://www.iso.org/standard/68235.html>.

Manuscript received: 29.09.2024